JBC Papers in Press. Published on August 9, 2004 as Manuscript M407368200

Proteomic Profiling of Bone Marrow Mesenchymal Stem Cells Upon TGF-β Stimulation

Daojing Wang[1] *, Jennifer S. Park [2], Julia S.F. Chu[2], Ari Krakowski[3], Kunxin Luo[3], David J. Chen[1], Song Li [2] *

[1] Life Sciences Division, Lawrence Berkeley National Laboratory, 1 Cyclotron Road, MS 84-171, Berkeley, CA 94720

[2] Department of Bioengineering, University of California, Berkeley, Berkeley, CA 94720-1762

[3] Department of Molecular and Cell Biology, University of California, Berkeley, 237 Hildebrand Hall, Berkeley, CA 94720-3206

*Correspondence to:

Daojing Wang, Ph.D.
Life Sciences Division
Lawrence Berkeley National Laboratory
1 Cyclotron Road, MS 84-171
Berkeley, CA 94720
Email: djwang@lbl.gov

Song Li, Ph.D.
Department of Bioengineering
University of California, Berkeley
471 Evans Hall
Berkeley, CA 94720-1762
Email: songli@socrates.berkeley.edu

Running Title: Proteomic profiling of MSCs upon TGF-β stimulation

SUMMARY

Bone marrow mesenchymal stem cells (MSCs) can differentiate into different types of cells, and have tremendous potential for cell therapy and tissue engineering. Transforming growth factor β1 (TGF-β) plays an important role in cell differentiation and vascular remodeling. We showed that TGF-β induced cell morphology change and an increase in actin fibers in MSCs. To determine the global effects of TGF-β on MSCs, we employed a proteomic strategy to analyze the effect of TGF-β on the human MSC proteome. By using two-dimensional gel electrophoresis and electrospray ionization coupled to Quadrupole/time-of-flight tandem mass spectrometers, we have generated a proteome reference map of MSCs, and identified ~30 proteins with an increase or decrease in expression or phosphorylation in response to TGF-β. The proteins regulated by TGF-β included cytoskeletal proteins, matrix synthesis proteins, membrane proteins, metabolic enzymes, etc. TGF-β increased the expression of smooth muscle (SM) α-actin and decreased the expression of gelsolin. Over-expression of gelsolin inhibited TGF-β-induced assembly of SM α-actin; on the other hand, knocking down gelsolin expression enhanced the assembly of α-actin and actin filaments without significantly affecting α-actin expression. These results suggest that TGF-β coordinates the increase of α-actin and the decrease of gelsolin to promote MSC differentiation. This study demonstrates that proteomic tools are valuable in studying stem cell differentiation and elucidating the underlying molecular mechanisms.

KEYWORDS: bone marrow mesenchymal stem cells; proteomic analysis; 2D gel electrophoresis; mass spectrometry; SM α-actin; gelsolin

INTRODUCTION

Bone marrow is one of the most abundant sources for adult stem cells. Bone marrow mesenchymal stem cells (MSCs) are non-hematopoietic and pluripotent stromal cells derived from bone marrow. MSCs can be expanded in culture, and differentiate into a variety of cell types such as osteoblasts, chondrocytes, adipocytes, skeletal muscle cells and smooth muscle cells (SMCs) in response to different microenvironmental cues (1-7). MSCs transplanted into the heart can differentiate into SMCs and contribute to the remodeling of vasculature (8,9). However, the effects of vascular microenvironmental factors on MSC differentiation into SMCs and the underlying molecular mechanisms are not well understood.

Transforming growth factor-β1 (TGF-β) proteins are multifunctional proteins that regulate cell growth, differentiation, migration and extracellular matrix production (10-14). It is recently shown that TGF-β increases smooth muscle (SM) α-actin expression in MSCs (15). In contrast, TGF-β induces chondrogenic differentiation of MSCs in the presence of dexamethasone or three-dimensional cell aggregates (16,17). These results indicate that the effects of TGF-β on MSC differentiation depend on other microenvironmental factors. To elucidate the molecular mechanism in TGF-β-induced MSC differentiation, we investigated the TGF-β-induced proteome changes in MSCs.

Proteome, the entire protein complement of the genome, determines cell phenotype and functions. With conventional molecular biological approaches, studies on the regulation of protein expression and activity can only be conducted on a limited number of proteins and on a protein-by-protein basis. Proteomics provides a systematic approach for the quantitative and qualitative mapping of the whole proteome (18,19). Rapid technology developments in two-dimensional electrophoresis (2DE), capillary/nano-high-pressure liquid chromatography (HPLC), mass spectrometry (MS), bioinformatics and protein microarrays have greatly advanced proteome characterization and biomarker discovery (18,20-24). 2DE separates proteins by isoelectric focusing (IEF) and sodium dodecylsulfate polyacrylamide gel electrophoresis (SDS-PAGE). 2DE offers better visualization of the whole proteome and hence the ease of subsequent

comparison and characterization, in addition to its lower cost. To date, 2DE still remains the central technology in proteomics for separation and differential comparison of thousands of proteins in a complex mixture (21,25,26). Proteins separated by 2DE can be digested and analyzed by MS, e.g., using matrix-assisted laser desorption ionization (MALDI) or electrospray ionization (ESI) coupled to quadrupole/time-of-flight (Q-TOF) mass analyzers or triple-quadrupole tandem mass spectrometers (MS/MS). MS/MS spectra can be used to determine the peptide sequence with high specificity (18,22).

In this study, we used ESI-MS/MS to identify proteins in 2D gels. A preliminary 2D reference map of MSCs was generated, and about 30 TGF-β-regulated proteins with changes at the expression level and/or posttranslational modifications were identified. We showed that TGF-β coordinated the increase of SM α-actin and the decrease of gelsolin to promote the assembly of α-actin and actin filaments in MSCs. These results from proteomic profiling will not only provide insight into the global responses of MSCs to TGF-β stimulation, but will also lead to in-depth studies on the mechanisms of proteomic changes in MSCs.

EXPERIMENTAL PROCEDURES

Cell Culture

Human bone marrow MSCs were obtained from Cambrex Corp (Walkersville, MD). These MSCs had been well characterized by their surface markers and differentiation potential. They are positive for CD105, CD166, CD29, and CD44, but negative for CD34, CD14, and CD45. MSCs were cultured in MSCGM medium with pre-screened fetal bovine serum (Cambrex Corp.) to allow for cell proliferation without differentiation. The cells were maintained in humidified incubators at 37^{o}C with 5% CO_2. Cell culture products and other consumable laboratory supplies were purchased from Fisher Scientific Corp. (Fairlawn, NJ) and VWR International (Brisbane, CA). MSCs up to passage 10 were used in our experiments.

Flow Cytometry

To confirm MSCs maintain their phenotype after expansion in culture, the cells were subjected to flow cytometry analysis. The cells were detached by trypsin treatment, followed by centrifugation and washing with PBS. After resuspension of the cells, the non-specific binding sites were blocked by incubation with 1% bovine serum albumin (Sigma) for 30 min. For primary antibodies conjugated with FITC (CD14, CD34, CD45, CD105, CD166), the samples were incubated with the primary antibody for 30 min, and the expression level of each surface marker was quantified by using a Beckman-Coulter EPICS XL flow cytometer. For primary antibodies without FITC conjugation (CD29 and CD44), the samples were incubated with an antibody against each of the surface markers for 30 min, and stained with a FITC-conjugated secondary antibody (Molecular Probes, Eugene, OR) for 30 min, followed by flow cytometry analysis. As negative controls, cells were incubated only with the FITC-conjugated secondary antibody. The antibodies against the surface markers CD14 and CD45 were from Santa Cruz Biotechnologies (Santa Cruz, CA). CD34 antibody was from BD Biosciences (San Jose, CA).

CD29 and CD105 antibodies were from Chemicon (Temecula, CA). CD166 antibody was from Serotec (Raleigh, NC). CD44 antibody was from Biosource (Camarillo, CA).

Chemicals and TGF-β Treatment

Chemicals were purchased from Sigma-Aldrich Corp. (St. Louis, MO) unless otherwise specified. TGF-β1 (Sigma-Aldrich Corp.) at 10 ng/ml was used to treat MSCs. Our pilot experiments showed that TGF-β1 at 5 ng/ml and 20 ng/ml induced similar level of SM α-actin and collagen I expression in MSCs. For long-term culture, TGF-β1 was supplemented when cultured medium was changed (every 2-3 days).

Cell Staining and Microscopy

The phase contrast images of MSC morphology were collected by using a Nikon inverted microscope (TE300) with 10x objective and a Hamamatsu Orca100 cooled digital CCD camera. The images were transferred directly from a frame grabber to the computer storage using C-Imaging System software (Compix Inc., Cranberry Township, PA).

Immunostaining and confocal microscopy were used to determine the subcellular distribution and organization of the proteins. MSCs were fixed in 4% paraformaldehyde in phosphate buffer saline (PBS) for 15 min, followed by permeabilization with 0.5% Triton X-100 in PBS for 10 min. For immunostaining, the specimens were incubated with the primary antibody against gelsolin (from BD Biosciences, Inc., San Jose, CA), α-actin or Flag-tag (Sigma-Aldrich Corp.) for 2 hr, and with FITC- or Rhodamine-conjugated secondary antibody (Jackson ImmunoResearch, West Grove, PA) for 1 hr. To stain F-actin filaments, the specimen was incubated with rhodamine-phalloidin for 30 min, followed by confocal microscopy. The images of the specimen were collected as Z-series sections with a Leica TCL SL confocal microscopy system equipped with argon and He/Ne laser sources, a scanner, and a Leica DM IRB

microscope. Multiple sections (0.3-μm thick for each section) were projected onto one plane for presentation.

Immunoblotting Analysis of Proteins

To prepare cell lysates for SDS-PAGE, the cells were lysed in a lysis buffer containing 25 mM Tris, pH 7.4, 0.5 M NaCl, 1% Triton X-100, 0.1% SDS, 1 mM PMSF, 10 μg/ml leupeptin and 1 mM Na_3VO_4. The lysates were centrifuged at 12,000 rpm by using a microfuge, and the protein concentration of the supernatants was measured by using a DC Protein Assay (Bio-Rad Laboratories, Hercules, CA). The proteins were run in SDS-PAGE and transferred to a nitrocellulose membrane, which was blocked with 3% nonfat milk and incubated with the primary antibody in TTBS buffer (25 mM Tris-HCl, pH 7.4, 60 mM NaCl, and 0.05% Tween 20) containing 0.1% bovine serum albumin. The bound primary antibodies were detected by using a goat anti-mouse or a goat anti-rabbit IgG-horseradish peroxidase conjugate (Santa Cruz Biotechnologies, Santa Cruz, CA) and the ECL detection system (Amersham Biosciences, Piscataway, NJ). The immunoblotting results were scanned with a HP high-resolution scanner, and the intensity of protein bands were quantified using NIH Image software.

The monoclonal antibody against gelsolin was from BD Biosciences Inc. The antibodies against actin (including all isoforms) and tubulin were from Santa Cruz Biotechnologies. The antibodies against α-actin (monoclonal) and Flag-tag (polyclonal) were from Sigma-Aldrich Corp. The antibody against HSP27 was from Stressgen Biotechnologies Corp (Victoria, BC, Canada).

Cell Lysis and 2D Gel Electrophoresis

Cells were washed three times using ice-cold PBS buffer and centrifuged down at 3000 rpm for 5 min. Residual PBS buffer on top was removed by careful pipetting. Cells were then disrupted with lysis buffer, which is a cocktail of 7M Urea, 2M thiourea, 4% 3-[(3-cholamidopropyl)dimethylammonio]-1-propanesulfonate (CHAPS), 40 mM

tris(hydroxymethyl)aminomethane (Tris base) and 20 mM DTT. Normally 1 ml of lysis buffer was used for 1-2 x 10^7 cells. Upon addition of lysis buffer, cells were immediately pipetted up and down several times to mix well. Samples were let stand at room temperature for about 1 hr and vortexed occasionally. They were transferred to Beckman thick wall tubes (#362305) and centrifuged at 66,000 rpm (100,000 g) in a Beckman TLA100.4 rotor for 30 min at 20ºC. Supernatant were aliquoted into siliconized tubes (PGC Scientifics, Frederick, MD) and stored at –80ºC. Modified Bradford assay (Bio-Rad Laboratories) was used to quantify the total protein amount in the cell lysates.

The first-dimension IEF was performed using an Amersham Ettan IPGphor unit with a power supply EPS 3501XL. Pre-cast 18 cm pH 3-10 NL IPG strips were obtained from Amersham Biosciences. 100 μg of lysate mixtures in triplicates were supplemented with rehydration solution (7 M urea, 2 M thiourea, 2% CHAPS, trace of bromophenol blue, 20 mM DTT and 0.5 % corresponding IPG buffer) to a final volume of 350 μl. IPG strips were then rehydrated with the sample mixture in a strip holder for 24 hr. IEF was carried out in three steps under step-n-hold mode: (i) 500 V, 1.0 hr; (ii) 1000 V, 3 hr; (iii) 8,000 V, 8 hr. The total voltage-hour (Vh) applied was 67,000. The second-dimension (SDS-PAGE) was carried out in an Ettan DALTsix system (Amersham Biosciences). IPG strips were equilibrated in two consecutive steps: (i) 30 min in 10 mg/ml of DTT; (ii) 30 min in 25 mg/ml of iodoacetamide (IAA) (Sigma-Aldrich Corp.), both dissolved in SDS equilibration buffer (50 mM Tris base, 6M urea, 30% glycerol (v/v), 2% SDS (w/v) and trace bromophenol blue). 1 mm-thick 10% polyacrylamide gels with a dimension of 27.5 cm x 21 cm were cast with 30% Duracryl, 0.65% Bis (Genomic Solutions, Ann Arbor, MI), 10% SDS, 10% ammonium persulfate and 0.375 M Tris buffer at pH 8.8. IPG strips were sealed on the top of gels with 0.5 % SeaKem LE Agarose (Cambrex Corp.). SDS-PAGE was performed at a constant voltage of 100 V at 10ºC and stopped once the bromophenol blue front disappeared from the gel.

Silver Staining and Image Analysis

Proteins on gels were visualized using silver staining performed with minor modifications to published procedures (27). Briefly, gels were fixed in 50% methanol/5% acetic acid for at least 2 hr followed by 20 min washing in 50% methanol. Gels were washed twice with ddH_2O for 15 min, treated with 0.02% $Na_2S_2O_3$ for 3 min, and rinsed twice with ddH_2O for 1 min before incubation in 0.1% silver nitrate for 30 min. After silver staining gels were rinsed twice with ddH_2O for 2 min, and shaken vigorously in developer containing 0.04% formalin (37% formaldehyde in water) and 2% Na_2CO_3. After 30 seconds, developer was discarded and gels were shaken in fresh developer until desired intensity was attained (approximately 3 min). Incubation in 5% acetic acid for 5 min terminated development after which gels were rinsed three times with ddH_2O for 2 min prior to imaging. For long-term storage, gels were incubated with 1% acetic acid at 4ºC.

Stained gels were imaged with an Umax PowerLook 1100 scanner (Umax Technologies, Dallas, TX) with a defined scan resolution of 250 dpi in the transmissive and gray blue mode. Protein expression with and without TGF-β treatment was compared using Z3 3.0 software (Compugen, Tel Aviv, Israel). All gel images were cropped to the same dimensions and auto-contrasted in Photoshop 7.0 prior to image analysis. Multiple gel analysis (MGA) wizard was applied to compare the two groups of three gels each. Spot detection and matching were achieved automatically initially and fine-tuned by manual registration. Spurious spots were excluded by manual annotation. To define spots with differential expression, the settings used were: spot contrast of 8, minimum confidence level of 0.95 and minimum spot area (pixels) of 50. Protein spots that were determined to be differentially expressed (n fold more than 2.0 or less than 0.5) using the automatic analyses were verified manually by local pattern comparison to exclude artifacts.

In-Gel Tryptic Digestion and Peptide Extraction

To identify differentially expressed proteins, the spots were excised from the gels

manually and digested with trypsin. Gel spots were diced into small pieces (1 mm^2) and placed into 0.65 mL siliconized tubes. 100 µL (or enough to cover) of 50 mM NH_4HCO_3 /50% ACN was added and the tube was vortexed for 10 min. After a brief spin the supernatant was discarded with gel-loading pipette tips. The washing step was repeated twice. Gel pieces were then brought to complete dryness with a Savant Speed Vac. 5 ng /µL trypsin (Promega, Madison, WI) freshly prepared in 50 mM NH_4HCO_3 was added to just barely cover the gel pieces. Trypsin solution added was about 3x volume of dry gel volume estimated and on average 20 µL was sufficient. The gel pieces were let stand to swell for 10 min under room temperature. They were then kept on ice for 30 min. Extra trypsin solution was discarded by pipetting to reduce trypsin autolysis. Finally 30 µL of 25 mM NH_4HCO_3 was gently overlaid on top and the tubes were incubated at 37°C overnight (16-20 hrs).

To extract the peptides from the gel pieces, 30 µL of ddH_2O was added and the tube was vortexed for 10 min followed by sonication in a water bath for 5 min. The aqueous portion was transferred to a clean siliconized tube. Peptides were further extracted with 30 µL of 50% ACN/5% formic acid twice and supernatants were combined. The total volume was reduced to approximately 5 µL by using Speed Vac. The resultant samples were then subjected to Q-TOF mass spectrometry directly or stored at –20ºC freezer for future analysis.

Protein Identification by LC-MS/MS

A hybrid Quadrupole/Orthogoanl Time-of-flight mass spectrometer Q-TOF API US (Waters, MA) interfaced with a capillary liquid chromatography system (Waters, MA) was used to carry out LC-MS/MS analysis. 1-2 µL of samples were injected through an auto-sampler into the LC system at the flow rate of 20 µL/min, and pre-concentrated on a 300 µm x 5 mm PepMap C18 precolumn (Dionex, CA). The peptides were then eluted onto a 75 µm x 15 cm PepMap C18 analytical column. The column was equilibrated with solution A (3% acetonitrile, 97% water, 0.1% formic acid) and the peptide separation was achieved with a solution gradient from 3% to 40% solution B (95% acetonitrile, 5% water, 0.1% formic acid), over 35 min at a flow rate of

250 nl/min. This flow rate through the column was reduced from 8 μL/min from pumps A and B by flow splitting.

The LC eluent was directed to the electrospray source with a PicoTip emitter (New Objectives, MA). The mass spectrometer was operated in positive ion mode with a source temperature of 100ºC and a cone voltage of 40 V. A voltage of 2 kV was applied to the PicoTip. TOF analyzer was set in the V-mode. The instrument was calibrated with a multi-point calibration using selected fragment ions from the collision-induced decomposition (CID) of Glu-fibrinopeptide B. MS/MS spectra were obtained in a data-dependent acquisition (DDA) mode in which the three multiple-charged (+2, +3, +4) peaks with the highest intensity in each MS scan were chosen for CID. Collision energies were set at 10 V and 30 V respectively during the MS scan and MS/MS scans.

Mass spectra were processed using MassLynx 4.0 software and proteins were identified using Protein Global Sever 1.0/2.0 software. The protein identities were further confirmed by Mascot (http://www.matrixscience.com) using the MS/MS peak lists exported from MassLynx. The non-redundant databases in the molecular weight range of 1,000-500,000 Da and pI between 3.0 and 10.0 were used at the website of The National Center for Biotechnology Information (NCBI). Modifications considered included carbamidomethylation of cysteine, N-terminal acetylation, N-terminal Gln to pyroGlu, oxidation of methionine and phosphorylation of serine, threonine and tyrosine.

RNA Isolation and Quantitative Polymerase-Chain-Reaction (qPCR)

Cells in each well in 6-well plates were lysed with 0.5 mL RNA Stat 60 (Tel-Test Inc, Friendswood, TX). RNA was extracted using chloroform and phenol extraction steps. Samples were centrifuged in between each of these steps for 15 min at 4^{o}C at 12000 rpm. Isopropanol was added to precipitate the RNA, and the samples were centrifuged for 30 min at the same conditions. 75% ethanol was added to wash the RNA pellet and centrifuged at 7500 rpm for 5

min. The pellet was resuspended in 20 μL DEPC-treated water and quantified using a RiboGreen® RNA quantification assay (Molecular Probes Inc, Eugene, OR).

Two-step reverse-transcription (RT)-PCR was performed using the ThermoScript RT-PCR system for first-strand cDNA synthesis (Invitrogen, Carlsbad, CA). The cDNA was made from equal amount of total RNA from each sample and qPCR was performed using SYBR-green kits and the ABI Prism® 7000 Sequence Detection System (Applied Biosystems, Foster City, CA) (28). Primers for SM α-actin, gelsolin and 18S were designed using the ABI Prism Primer Express™ software v.2.0 (Applied Biosystems). Complete genomic sequences and mRNA sequence were downloaded from NCBI website (http://www.ncbi.nlm.nih.gov/LocusLink) to identify the intron-exon junctions. The primers that span an exon-exon junction were used to ensure the specific amplification of cDNA. The sequences of the designed primers were used to BLAST against nucleotide sequences in the NCBI database (http://www.ncbi.nlm.nih.gov/BLAST/) to make sure that the primer sequences were unique. The primers used in this study are listed in Table 1.

After each experiment, the melting temperature and the dissociation curve of PCR products were obtained to confirm the product specificity. The amount of RNA for each gene was normalized with the amount of 18S RNA in the same sample.

Transfection of DNA Plasmids and Small Interfering RNA (siRNA)

PCR was used to engineer the Flag-tagged gelsolin construct by inserting the gelsolin cDNA beginning with the second codon immediately following the Flag nucleotide sequence (GACTACAAGGATGACGATGACAAG) in the pCMV5b vector.

MSCs were seeded in serum-free medium, and the DNA plasmids (2 μg for 10 cm^2 culture area) were transfected into MSCs using the lipofectAMINE PLUS reagent (Invitrogen). After incubation with the mixture of plasmids and lipofectAMINE reagents for 5 hr, the cells were cultured for 1 day, and treated with TGF-β or kept as control. The expression efficiency of DNA plasmids was about 20%.

SiRNA for gelsolin was from Dharmacon Inc (Lafayette, CO). The FITC-conjugated control siRNA was from Cell Signaling Technology Inc (Beverly, MA). The siRNAs (100 nM for 10 cm^2 culture area) were transfected into MSCs by using lipofectAMINE 2000. The transfection efficiency of siRNA was more than 90%.

RESULTS

Characterization of MSCs

We used MSCs up to passage 10 in our experiments. To confirm that expanded MSCs maintain their phenotype, MSCs were stained for a set of cell surface markers. As shown in Figure 1, MSCs at passage 10 were positive for CD105, CD166, CD29 and CD44, but were negative for CD14, CD45 and CD34, suggesting that expanded MSCs maintain their phenotype. To further prove that expanded MSCs had pluripotent differentiation potential, MSCs at passage 10 were tested for the differentiation into chondrocytic cells and osteogenic cells by following the instructions from the manufacturer. MSCs cultured as a three-dimensional pellet in chondrogenic media for two weeks showed a round shape and synthesized large amounts of glycosaminoglycans, suggesting the differentiation of MSCs into chondrocytic cells (data not shown). MSCs in osteogenic media for two weeks showed matrix mineralization by Alizarin Red stain (data not shown), suggesting the differentiation of MSCs into osteogenic cells.

TGF-β Induced Morphological Changes, Increases Actin Filaments and Increased SM α–actin Expression

Long-term treatment of MSCs with TGF-β significantly changed the cell morphology. As shown in Figure 2, 2 days after TGF-β treatment, MSCs have a more spread-out and myoblast-like morphology, and intracellular fibrous structures were visible (indicated by arrows in Figure 2B). This cell morphology was maintained as the cells grew and reached confluence after 6 days (Figure 2F).

To determine whether the intracellular fibrous structure was actin cytoskeleton, MSCs were stained on actin filaments. Indeed, MSCs treated by TGF-β for 4 days showed more actin filaments and thick fibers (Figure 3). To determine whether TGF-β regulated the amount of actin, immunoblotting analysis was performed. As shown in Figure 3C, TGF-β specifically increased α-actin expression without significantly affecting total actin amount. Tubulin expression was used as an internal control to show equal loading of the protein samples. At the

transcription level, TGF-β increased the gene expression of SM α-actin and SM-22α (data not shown). These results suggest that TGF-β may promote the expression of SM contractile markers in MSCs.

TGF-β Induced Proteome Changes in MSCs

Although the effects of TGF-β on various cell types have been widely studied, the effect of TGF-β on MSCs has not been investigated comprehensively. We used a proteomic approach to profile the TGF-β-induced protein expression and modifications. The proteins in the cell lysates were separated by 2DE, followed by silver staining. A representative 2D gel image of protein lysates from MSCs without TGF-β treatment is shown in Figure 4. About 1500 protein spots were resolved and identified with high confidence (>95%). Overall around 60 protein spots were found consistently up- or down-regulated by over two-folds in triplicate experiments after TGF-β treatment for 4 days. We have made an initial effort to identify around 30 protein spots, encompassing a wide range of molecular weights, pIs, fold changes and abundance. All 30 protein spots were identified successfully with high confidence using in-gel trypsin digestion followed by tandem mass spectrometry as described in Materials and Methods. The location of each spot is labeled with a number and an arrow indicating up-(upward) or down-(downward) regulation by TGF-β. The predicted molecular weights and isoelectric points of un-modified proteins using the Z3 program agree well with their theoretical values (± 10%).

Proteins identified so far are listed in Table 2, grouped according to their primary functions. For all the proteins identified, two search engines (ProteinLynx and Mascot) gave the same protein hits with high confident scores and at least two peptides sequenced with good MS/MS spectra. The majority of these spots has an n-fold value either bigger than 2 or smaller than 0.5, defined as differentially expressed previously. Two actin spots #1324 and #1032 and one heat shock protein 27 (HSP27) spot # 1018 were also identified as reference spots. For spot #1116 and #1030, more than one protein was identified without ambiguity, suggesting co-migration of these proteins. These TGF-β regulated proteins are involved in a variety of cellular

processes. They include cytoskeleton proteins (i.e. gelsolin and T-plastin), cell membrane proteins (i.e. annexin A2), proteins involved in matrix synthesis (i.e. collagen binding protein 2 or CBP2), metabolic enzymes (i.e. thioredoxin reductase), protein synthesis and degradation (i.e. T-complex protein 1 and proteasome subunit) and stress response proteins (i.e. HSP27), etc. In addition, TGF-β not only modulates protein expression levels, but also post-translational modifications, e.g., HSP27 phosphorylation at Ser-82 (data not shown). The TGF-β-induced change in SM α-actin and gelsolin expression were further investigated as described in the following sections.

TGF-β Coordinated the Increase of SM α-actin and the Decrease of Gelsolin in MSCs

As shown in Figure 5A, Spot #1394 had lower level after TGF-β treatment. This protein was identified as gelsolin, an actin severing protein. Gelsolin has been shown to regulate actin structure, cell motility and apoptosis (29,30), but the role of gelsolin in cell differentiation is not clear. To determine the time course of gelsolin expression in response to TGF-β, immunoblotting analysis was performed. As in Figure 5B, TGF-β significantly decreased gelsolin expression after 4 days and 6 days.

To determine whether TGF-β regulated the expression of gelsolin and α-actin at transcription level, we examined the gene expression at the earlier time points with qPCR (Figure 6). After 24 hr of TGF-β treatment, the gene expression of gelsolin decreased by 50% while α-actin expression increased by 4 folds. After 48 hr, the gene expression of gelsolin and α-actin showed same trend as that at 24 hr, suggesting the TGF-β-induced protein expression change is sustained. These results indicate that TGF-β coordinated the increase of SM α-actin expression and the decrease of gelsolin expression at transcriptional level.

To determine the spatial relationship between gelsolin and actin filaments in MSCs, cells with or without TGF-β treatment for 4 days were double-stained for gelsolin and actin filaments (Figure 7). Gelsolin mostly co-localized with actin filaments except for a weak background in the cytoplasm. TGF-β decreased gelsolin staining and the co-localization of gelsolin with actin

cytoskeleton, and increased actin filaments in MSCs. In local areas where the gelsolin level was low (indicated by arrows in Figure 7B), more actin filaments were assembled (indicated by arrows in Figure 7D), suggesting that the decrease of gelsolin is correlated with the increased actin filament assembly. Double staining for gelsolin and SM α-actin showed the same results (data not shown).

The Decrease of Gelsolin Enhanced the Assembly of α-actin and Actin Filaments, But Did Not Affect the Expression of α-actin

To directly determine whether the increase of gelsolin expression would inhibit TGF-β-induced α-actin assembly into actin filaments, we over-expressed the Flag-tagged gelsolin in MSCs, and treated the cells with TGF-β for two days. As shown in Figure 8, over-expression of gelsolin (Figure 8A and 8B) significantly decreased the incorporation of SM α-actin into actin filaments in comparison with non-transfected cells in the same field (Figure 8C and 8D respectively). TGF-β increased actin filaments containing α-actin in non-transfected cells, but this increase was blocked in cells over-expressing gelsolin (Figure 8D). These results suggest that the decrease of gelsolin is required for TGF-β-induced α-actin assembly into filaments.

Since actin polymerization had been shown to increase SM α-actin expression (31), we determined whether the decrease of gelsolin expression would increase actin polymerization thus enhancing the expression of SM α-actin. To test this possibility, gelsolin siRNA was used to knock down the expression level of gelsolin in MSCs to mimic the decrease of gelsolin expression by TGF-β. The transfection efficiency of siRNA in MSCs was more than 90% (Figure 9A), which allowed us to analyze the gene and protein expression in the whole cell population. As shown in Figure 9B, transfection of control siRNA did not affect gelsolin levels, while gelsolin siRNA suppressed gelsolin mRNA levels by more than 80% after 1 day. Since the gelsolin protein level was related to many factors such as protein half-life and degradation rate, the protein level of gelsolin did not show a significant change within 2 days, but was decreased dramatically by gelsolin siRNA transfection after 4 and 6 days. However, based on

immunoblotting, there was no significant change of α-actin protein level at any time points. These results suggest that the decrease of gelsolin expression does not significantly regulate α-actin expression.

To determine whether the decrease of gelsolin expression was sufficient to enhance α-actin assembly into actin filaments, MSCs were transfected with gelsolin siRNA, and stained on F-actin and α-actin. As shown in Figure 10, knocking down gelsolin increased actin filaments (Figure 10A-B), and enhanced α-actin assembly into filaments (Figure 10C-D).

DISCUSSION

A major challenge in the post-genomic era is to decipher the temporal and spatial functions and interactions of proteins in a cell. Although still in its development stage, proteomic profiling is poised to play an essential role in this endeavor. Proteome-wide screening may identify unique markers and elucidate interconnections between different cellular signaling pathways. In this study, we have profiled for the first time the global protein expression in human bone marrow MSCs upon TGF-β stimulation. In combination with more traditional biochemical/biophysical methods such as western blotting and microscopy, we have gained important insights into the mechanisms of TGF-β-regulation of MSCs. Using a proteomic approach, we have generated the first 2D reference map for MSCs. This 2D reference map of MSCs will facilitate future studies on MSC functions and differentiation in response to various environmental factors. Based on this map, higher-resolution proteome maps of MSCs with pre-fractionated cell lysates and zoom-in pI range 2D gels can be generated. The information obtained from proteomic profiling will help us to elucidate connections between broad cellular pathways/molecules that were neither apparent nor predictable through traditional biochemical analysis in the past.

We showed that TGF-β induced a sustained increase of SM α-actin expression in MSCs (Figure 3). This is consistent with the role of TGF-β in angiogenesis and vasculogenesis. It has been shown that TGF-β can enhance SMC differentiation and the recruitment of SMCs to the newly formed blood vessels (32). However, TGF-β induces chondrogenic differentiation of MSCs in the presence of dexamethasone or three-dimensional cell aggregates (16,17). These results suggest that TGF-β-induced responses in MSCs are context-dependent, e.g., dependent on cell-cell adhesion, other chemical factors and mechanical factors in the microenvironment. There is evidence that TGF-β-mediated signaling pathways can crosstalk with mechanical force-induced signaling and gene expression in vascular cells (33,34). For example, for SMCs cultured in a collagen scaffold, TGF-β stimulates the expression of SM α-actin, which is further enhanced

by mechanical strain (33). It is possible that mechanical strain and TGF-β may collaborate to induce MSC differentiation into mature SMCs.

A significant finding from this study is that TGF-β coordinates the expression of gelsolin and α-actin to promote the differentiation of MSCs (Figures 3, 5-7) and that the decrease of gelsolin is necessary and sufficient for the assembly of α-actin and actin filaments induced by TGF-β (Figures 8-10). Gelsolin, a protein originally identified as an actin severing protein, has been shown to regulate actin structure, cell motility and apoptosis (29,30). To our knowledge, this is the first report on the regulation of gelsolin expression by TGF-β. Whether this mechanism is MSC-specific and whether the gelsolin pathway synergizes with other muscle specific pathways remain to be determined. It is interesting that the decrease of gelsolin in MSCs enhanced the assembly of SM α-actin into actin filaments at the post-translational level (Figures 8 and 10) but did not affect the protein expression of α-actin (Figure 9). In SMCs, TGF-β increases α-actin gene expression through a TCE element by decreasing KLF4 expression and increasing KLF5 expression (35-37). In addition, TGF-β enhances serum-response factor (SRF) expression/activity and SM marker expression through a CArG element (35,38). Actin polymerization has been shown to increase SRF activity and thus α-actin expression (31). In our system, the down-regulation of gelsolin expression by TGF-β increases actin filament assembly (Figures 3 and 7), which could in turn activate SRF to increase α-actin expression at the transcriptional level. However, knocking down gelsolin did not significantly affect α-actin expression. One explanation is that the basal level of actin polymerization was sufficient to maintain SRF activity and that the further increase of actin polymerization by decreasing gelsolin would not enhance SRF activity. Alternatively, other factors such as KLFs could play important roles in α-actin expression in MSCs.

Interestingly, TGF-β also regulates other molecules involved in actin organization. HSP27 has multiple phosphorylated isoforms (39) and mediates actin polymerization at the downstream of p38 MAPK pathway (40). Our results indicate a decrease of HSP27 phosphorylation at Ser-82 after TGF-β stimulation (Table 2). TGF-β also decreased T-plastin

(fimbrin) expression in MSCs (Table 2). T-plastin is normally found in epithelial and mesenchymal cells, and is an actin-bundling protein regulating microvilli actin filaments (41-43). The functional consequence of HSP27 de-phosphorylation and T-plastin down-regulation needs further investigation.

It needs to be pointed out that some proteome changes induced by TGF-β in MSCs may be cell-type specific, while some may be ubiquitous (e.g. CBP2). The distinction between these two cases needs further investigations. The proteomic profiling allowed us to identify many novel targets and effectors of TGF-β induced signaling. The data derived from this study will lead to more focused and in-depth research on the effects of TGF-β on cellular functions and MSC differentiation. The information obtained from this study will not only have significant impact on stem cell biology, but also have profound implications in stem cell therapy and tissue regeneration. MSCs have tremendous potential as a cell source for cell transplantation and tissue engineering. The knowledge of MSC responses to environmental factors such as TGF-β will help us to understand MSC differentiation *in vivo*, e.g., participation of tissue regeneration in ischemic heart after transplantation, and provide a rational basis for stem cell engineering, e.g., to optimize *in vitro* culture conditions to expand MSCs and control MSC differentiation for tissue engineering applications.

ACKNOWLEDGMENT

The gelsolin cDNA was a generous gift from Dr. Alan Lader in the Hematology Division at Brigham and Women's Hospital in Boston, MA. This study was supported by a Berkeley start-up fund (S.L.) and a grant from National Heart, Lung and Blood Institute (HL079419). D.W. acknowledges the financial support from Dr. Pricilla K. Cooper.

REFERENCES

1. Caplan, A. I., and Bruder, S. P. (2001) *Trends Mol Med* **7**, 259-264

2. Wakitani, S., Saito, T., and Caplan, A. I. (1995) *Muscle Nerve* **18**, 1417-1426

3. Ferrari, G., Cusella-De Angelis, G., Coletta, M., Paolucci, E., Stornaiuolo, A., Cossu, G., and Mavilio, F. (1998) *Science* **279**, 1528-1530

4. Jiang, Y., Jahagirdar, B. N., Reinhardt, R. L., Schwartz, R. E., Keene, C. D., Ortiz-Gonzalez, X. R., Reyes, M., Lenvik, T., Lund, T., Blackstad, M., Du, J., Aldrich, S., Lisberg, A., Low, W. C., Largaespada, D. A., and Verfaillie, C. M. (2002) *Nature* **418**, 41-49

5. Galmiche, M. C., Koteliansky, V. E., Briere, J., Herve, P., and Charbord, P. (1993) *Blood* **82**, 66-76

6. Pittenger, M. F., Mackay, A. M., Beck, S. C., Jaiswal, R. K., Douglas, R., Mosca, J. D., Moorman, M. A., Simonetti, D. W., Craig, S., and Marshak, D. R. (1999) *Science* **284**, 143-147

7. Prockop, D. J. (1997) *Science* **276**, 71-74

8. Gojo, S., Gojo, N., Takeda, Y., Mori, T., Abe, H., Kyo, S., Hata, J., and Umezawa, A. (2003) *Exp Cell Res* **288**, 51-59

9. Mangi, A. A., Noiseux, N., Kong, D., He, H., Rezvani, M., Ingwall, J. S., and Dzau, V. J. (2003) *Nat Med* **9**, 1195-1201

10. Topper, J. N. (2000) *Trends Cardiovasc Med* **10**, 132-137

11. Massague, J., and Wotton, D. (2000) *Embo J* **19**, 1745-1754

12. Moustakas, A., Souchelnytskyi, S., and Heldin, C. H. (2001) *J Cell Sci* **114**, 4359-4369

13. Roberts, A. B. (1998) *Miner Electrolyte Metab* **24**, 111-119

14. Derynck, R., and Zhang, Y. E. (2003) *Nature* **425**, 577-584

15. Kinner, B., Zaleskas, J. M., and Spector, M. (2002) *Exp Cell Res* **278**, 72-83

16. Johnstone, B., Hering, T. M., Caplan, A. I., Goldberg, V. M., and Yoo, J. U. (1998) *Exp Cell Res* **238**, 265-272

17. Mackay, A. M., Beck, S. C., Murphy, J. M., Barry, F. P., Chichester, C. O., and Pittenger, M. F. (1998) *Tissue Eng* **4**, 415-428

18. Patterson, S. D., and Aebersold, R. H. (2003) *Nat Genet* **33 Suppl**, 311-323

19. Blackstock, W. P., and Weir, M. P. (1999) *Trends Biotechnol* **17**, 121-127

20. Mo, W., and Karger, B. L. (2002) *Curr Opin Chem Biol* **6**, 666-675

21. Rabilloud, T. (2002) *Proteomics* **2**, 3-10

22. MacCoss, M. J., and Yates, J. R., 3rd. (2001) *Curr Opin Clin Nutr Metab Care* **4**, 369-375

23. Yarmush, M. L., and Jayaraman, A. (2002) *Annu Rev Biomed Eng* **4**, 349-373

24. Srinivas, P. R., Verma, M., Zhao, Y., and Srivastava, S. (2002) *Clin Chem* **48**, 1160-1169

25. Witzmann, F. A., and Li, J. (2002) *Am J Physiol Gastrointest Liver Physiol* **282**, G735-741

26. Lilley, K. S., Razzaq, A., and Dupree, P. (2002) *Curr Opin Chem Biol* **6**, 46-50

27. Shevchenko, A., Wilm, M., Vorm, O., and Mann, M. (1996) *Anal Chem* **68**, 850-858

28. Li, S., Lao, J. M., Chen, B. P. C., Li, Y. S., Zhao, Y. H., Chu, J., Chen, K. D., Tsou, T. C., Peck, K., and Chien, S. (2002) *Faseb J* **16**, U346-U370

29. Kwiatkowski, D. J. (1999) *Curr Opin Cell Biol* **11**, 103-108

30. Sun, H. Q., Yamamoto, M., Mejillano, M., and Yin, H. L. (1999) *J Biol Chem* **274**, 33179-33182

31. Sotiropoulos, A., Gineitis, D., Copeland, J., and Treisman, R. (1999) *Cell* **98**, 159-169

32. Hirschi, K. K., Skalak, T. C., Peirce, S. M., and Little, C. D. (2002) *Ann N Y Acad Sci* **961**, 223-242

33. Stegemann, J. P., and Nerem, R. M. (2003) *Ann Biomed Eng* **31**, 391-402

34. Topper, J. N., Cai, J., Qiu, Y., Anderson, K. R., Xu, Y. Y., Deeds, J. D., Feeley, R., Gimeno, C. J., Woolf, E. A., Tayber, O., Mays, G. G., Sampson, B. A., Schoen, F. J., Gimbrone, M. A., Jr., and Falb, D. (1997) *Proc Natl Acad Sci U S A* **94**, 9314-9319

35. Hautmann, M. B., Madsen, C. S., and Owens, G. K. (1997) *J Biol Chem* **272**, 10948-10956

36. Adam, P. J., Regan, C. P., Hautmann, M. B., and Owens, G. K. (2000) *J Biol Chem* **275**, 37798-37806

37. Liu, Y., Sinha, S., and Owens, G. K. (2003) *J Biol Chem*

38. Hirschi, K. K., Lai, L., Belaguli, N. S., Dean, D. A., Schwartz, R. J., and Zimmer, W. E. (2002) *J Biol Chem* **277**, 6287-6295

39. Landry, J., Lambert, H., Zhou, M., Lavoie, J. N., Hickey, E., Weber, L. A., and Anderson, C. W. (1992) *J Biol Chem* **267**, 794-803

40. Hedges, J. C., Dechert, M. A., Yamboliev, I. A., Martin, J. L., Hickey, E., Weber, L. A., and Gerthoffer, W. T. (1999) *J Biol Chem* **274**, 24211-24219

41. Glenney, J. R., Jr., Kaulfus, P., Matsudaira, P., and Weber, K. (1981) *J Biol Chem* **256**, 9283-9288

42. Arpin, M., Friederich, E., Algrain, M., Vernel, F., and Louvard, D. (1994) *J Cell Biol* **127**, 1995-2008

43. Fath, K. R., and Burgess, D. R. (1995) *Curr Biol* **5**, 591-593

FIGURE LEGENDS

Figure 1. Flow cytometry analysis of cell surface markers in MSCs. As described in Experimental Procedure, MSCs at passage 10 were subjected to flow cytometry analysis after they were stained with FITC-conjugated CD14 or CD45 antibodies (top), FITC-conjugated CD34, CD105 or CD166 antibodies (middle), and monoclonal antibodies against CD29 or CD44.

Figure 2. Effect of TGF-β on MSC morphology. MSCs were kept as un-treated control (A, C and E) or treated with 10 ng/ml of TGF-β1 (B, D and F) for up to 6 days. Phase-contrast images were collected at different time points (Day 2, 4 and 6). Images were representatives of three experiments. The arrows in B indicate the fibrous structure in the cells. Bar=100 μm.

Figure 3. Effects of TGF-β on actin fibers and α-actin expression in MSCs. MSCs were kept as control (A) or treated with TGF-β (B) for 4 days, and stained for actin filaments using phalloidin. The scale bar in B is 100 μm. (C) MSCs were treated with TGF-β1 for 2, 4 and 6 days, and protein expression was analyzed by immunoblotting. The actin and tubulin bands show equal loading of proteins in each sample. The expression of α-actin in each sample was normalized with respective tubulin expression, and the ratios of normalized α-actin levels between TGF-β treated samples and controls at different time points were calculated. Bar graphs were mean±standard deviation (SD) of relative α-actin levels from three experiments. For statistical analysis, the data was log-transformed, and a one-sample t-test was performed. The asterisks (*) indicate significant difference between TGF-β-treated samples and the respective controls ($P<0.05$).

Figure 4. A 2D reference map for MSCs showing up- and down-regulated protein spots after TGF-β treatment for 4 days. MSCs were either kept as no-treatment control or treated with TGF-β for 4 days. The protein lysates were subjected to 2DE, followed by silver staining and image

analysis. Results were quantified from three sets of 2DE. A 2DE gel after silver staining (from a no-treatment control sample) is shown here as a representative. IEF (pH 3-10 non-linear gradient) is in the horizontal direction. PAGE (10% gel) is in the vertical direction. Except for spots #1324 and #1032 (actins with no significant change), upward arrows indicate up-regulation, and downward arrows indicate down-regulation. The spots of interest were excised from the gels and digested with trypsin. The resulting peptides were used for LC-MS/MS analysis, and the proteins were identified and listed in Table 2.

Figure 5. Effects of TGF-β on gelsolin expression in MSCs. (A) Identification of gelsolin in 2D gels. MSCs were kept as control or treated with TGF-β (10 ng/ml) for 4 days, and cell lysates were subjected to 2DE and silver staining. Spot #1394 showed decrease after TGF-β treatment, and was identified as gelsolin. (B) Protein expression of gelsolin in response to TGF-β. MSCs were treated with TGF-β for 2, 4 and 6 days, and protein expression was analyzed by immunoblotting. The actin and tubulin bands show equal loading of proteins in each sample. The expression of α-actin in each sample was normalized with respective tubulin expression, and the ratios of normalized α-actin levels between TGF-β treated samples and controls at different time points were calculated. Bar graphs were mean±SD of relative α-actin levels from three experiments. For statistical analysis, the data was log-transformed, and a one-sample t-test was performed. The asterisks (*) indicate significant difference between TGF-β-treated samples and the respective controls ($P<0.05$).

Figure 6. Gene expression of gelsolin and α-actin in response to TGF-β. MSCs were treated with TGF-β for 12, 24 and 48 hr, and the gene expression of gelsolin (in A), SM α-actin (in B) and the level of 18S RNA were analyzed by qPCR. The expression of gelsolin and α-actin was normalized by the level of 18S RNA in the respective sample. The relative gene expression (normalized with the respective control for each gene) is presented. Error bars represent SD from

three experiments. For statistical analysis, the data was log-transformed, and a one-sample t-test was performed. The asterisks (*) indicate significant difference between TGF-β-treated samples and the respective controls ($P<0.05$).

Figure 7. Effects of TGF-β on gelsolin and actin fibers. MSCs were either kept as untreated controls (A and C) or treated with TGF-β1 (B and D) for 4 days, and stained for gelsolin by using monoclonal mouse gelsolin antibody followed by FITC-anti-mouse secondary antibody (A and B) and actin filaments by using Rhodamine-phalloidin (C and D). The arrows in B and D indicate the area with less gelsolin but more actin fibers. Bar=100 μm.

Figure 8. Role of gelsolin in TGF-β-induced actin filament assembly. MSCs were transfected with Flag-gelsolin. One day after transfection, cells were kept as control (A and C) or treated with TGF-β1 (B and D) for two more days. Then the cells were fixed and double-stained for Flag-tag (A and B) and α-actin (C and D). Bar=50 μm.

Figure 9. Effect of knocking down gelsolin on α-actin expression. MSCs were transfected with gelsolin siRNA or control siRNA (conjugated with FITC), and used for microscopy, gene expression analysis and immunoblotting analysis. (A) To demonstrate the transfection efficiency, one day after transfection with control siRNA, each field was subjected to phase contrast and fluorescence microscopy, as shown by the representative field. Bar=100 μm. (B) One day after transfection, the samples were lysed for qPCR analysis of gelsolin gene expression. The expression of gelsolin in each sample was normalized with respective 18S RNA level, and normalized with the gelsolin expression in no-treatment control. Bar graphs were mean±SD from three experiments. For statistical analysis, the data was log-transformed, and a one-sample t-test

was performed. The asterisks (*) indicate significant difference when compared with no-treatment controls ($P<0.05$). (C) Immunoblotting analysis of gelsolin and α-actin protein expression after knocking down gelsolin.

Figure 10. Effect of knocking down gelsolin on actin filament assembly. MSCs were transfected with control siRNA (A and C) or gelsolin siRNA (B and D). Four days after transfection, cells were fixed and stained for F-actin (A and B) or α-actin (C and D), followed by confocal microscopy. Bar=50 μm.

Table 1. Primers used in qPCR

Gene Name	Forward Primer (5' to 3')	Reverse Primer (5' to 3')
SM α-actin	ACCCTGCTCACGGAGGC	GTCTCAAACATAATTTGAGTCATTTTCTC
Gelsolin	TTGACTTCTGCTAAGCGGTACATC	GGCTCAAAGCCTTGCTTCAC
18S	CGCAGCTAGGAATAATGGAATAGG	CATGGCCTCAGTTCCGAAA

Table 2. Proteins Identified in 2D Gel

Spot Number	TGF-β Induced Change (Fold)	Protein Name	SwissProt. Accession Number	Molecular Weight kDa (theoretical)	pI (theoretical-unmodified)
		Cytoskeleton Proteins			
1394	0.3	Gelsolin	P06396	85.7	6.2
1144	0.1	T-plastin (isoform)	P13797	70.4	5.50
1098	0.3	T-plastin	P13797	70.4	5.50
1324	1.0	γ-actin	P02571	41.8	5.31
1032	1.1	α-cardiac actin	P04270	42	5.23
		Cell Membrane-Bound Molecules			
1050	0.3	Annexin A6	P08133	75.7	5.42
2198	2.0	Annexin A2 (isoform)	P07355	38.5	7.56
2034	5.2	Annexin A2	P07355	38.5	7.56
		Proteins Involved in Matrix Synthesis			
3471	2.3	Collagen-binding protein 2 [Precursor]	P50454	46.4	8.75
1385	2.7	Collagen-binding protein 2 [Precursor](isoform)	P50454	46.4	8.75
1468 *	Unique	Collagen-binding protein 2 [Precursor](isoform)	P50454	46.4	8.75
		OR 47 kDa heat shock protein [precursor] (isoform)	P29043	46.3	8.27
		Metabolic Enzymes			
1176	0.1	Glyceraldehyde 3-phosphate dehydrogenase, liver	P04406	35.9	8.58
1776	0.3	Thioredoxin reductase	Q16881	54.4	6.1
1340	0.4	Malate dehydrogenase, cytoplasmic	P40925	36.3	6.89
1116 *	0.5	Tyrosyl-tRNA synthetase	P54577	59.1	6.61
		UDP-glucose 6-dehydrogenase	O60701	55.0	6.73
1106	2.3	Glucose-6-phosphate 1-dehydrogenase	P11416	59.1	6.44
1506	3.9	Pyruvate kinase, M2 isozyme	P14786	57.8	7.95
1680	4.8	Aldehyde dehydrogenase X, mitochondrial [precursor]	P30837	57.2	6.41
2114	4.9	Transaldolase	P37837	37.5	6.36
		Protein Synthesis and Degradation			
1146	0.4	T-complex protein 1, epsilon subunit	P48643	59.7	5.45
1230	0.3	Ubiquitin carboxyl-terminal hydrolase isozyme L1	P09936	24.8	5.33
2388	0.4	Proteasome subunit α type 2	P25787	25.9	7.5
		Others			
1178	0.5	Heat shock 27 kDa protein (phosphorylated at ser 82)	P04792	22.8	5.98
1018	1.3	Heat shock 27 kDa protein	P04792	22.8	5.98
1438	2.0	Programmed cell death 6 interacting protein	Q8WUM4	96	6.1
1388	2.0	Septin 6	Q14141	49.7	6.24
1338	0.3	Peroxiredoxin 2	P32119	21.9	5.66
1030 *	0.5	Chloride intracellular channel protein 4	Q9Y696	28.7	5.5
		Nicotinamide N-methyltransferase	P40261	29.5	5.6
		Vimentin (fragment)	P08670	53.6	5.1

Table 2. MSCs were either kept as no-treatment control or treated with TGF-β for 4 days. The protein lysates were subjected to 2DE, followed by silver staining and image analysis. Results were quantified from three sets of 2DE. The spots of interest were excised from the gels and digested with trypsin. The resulting peptides were used for LC-MS/MS analysis, and the proteins were identified by searching the databases using peptide sequences.

* Note: For spot #1468, the digested peptides from the spot were present in both collagen-binding protein 2 and HSP47 (these two proteins have 80% homologous sequences). This spot was only detected in TGF-β-treated samples (Unique). For spots #1116 and #1030, more than one protein was identified from the digested peptides, suggesting that these proteins co-migrated in the gels.

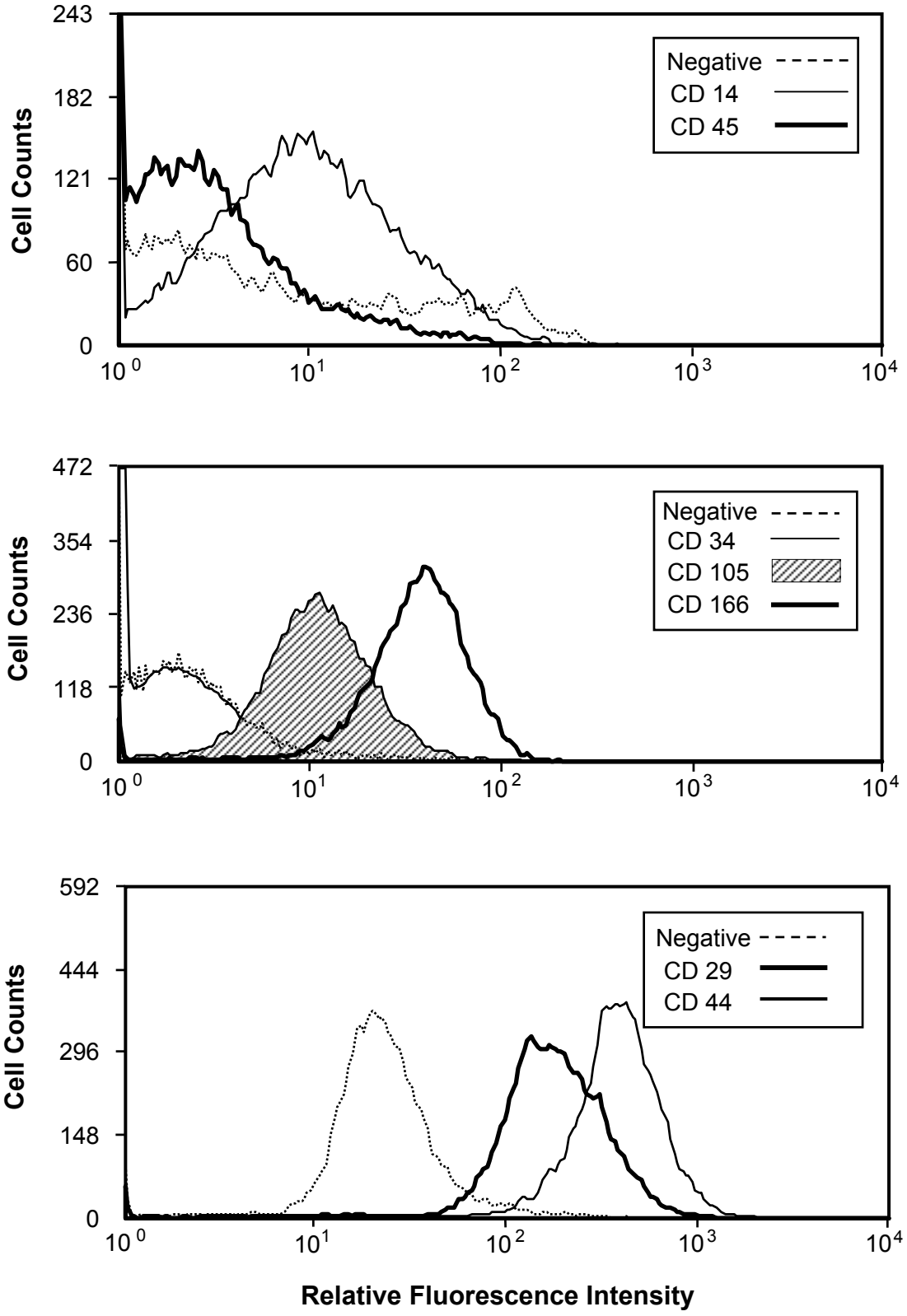
243
182
121
60
0
Cell Counts
Negative
CD 14
CD 45
10^0
10^1
10^2
10^3
10^4
472
354
236
118
0
Cell Counts
Negative
CD 34
CD 105
CD 166
10^0
10^1
10^2
10^3
10^4
592
444
296
148
0
Cell Counts
Negative
CD 29
CD 44
10^0
10^1
10^2
10^3
10^4
Relative Fluorescence Intensity

Figure 1

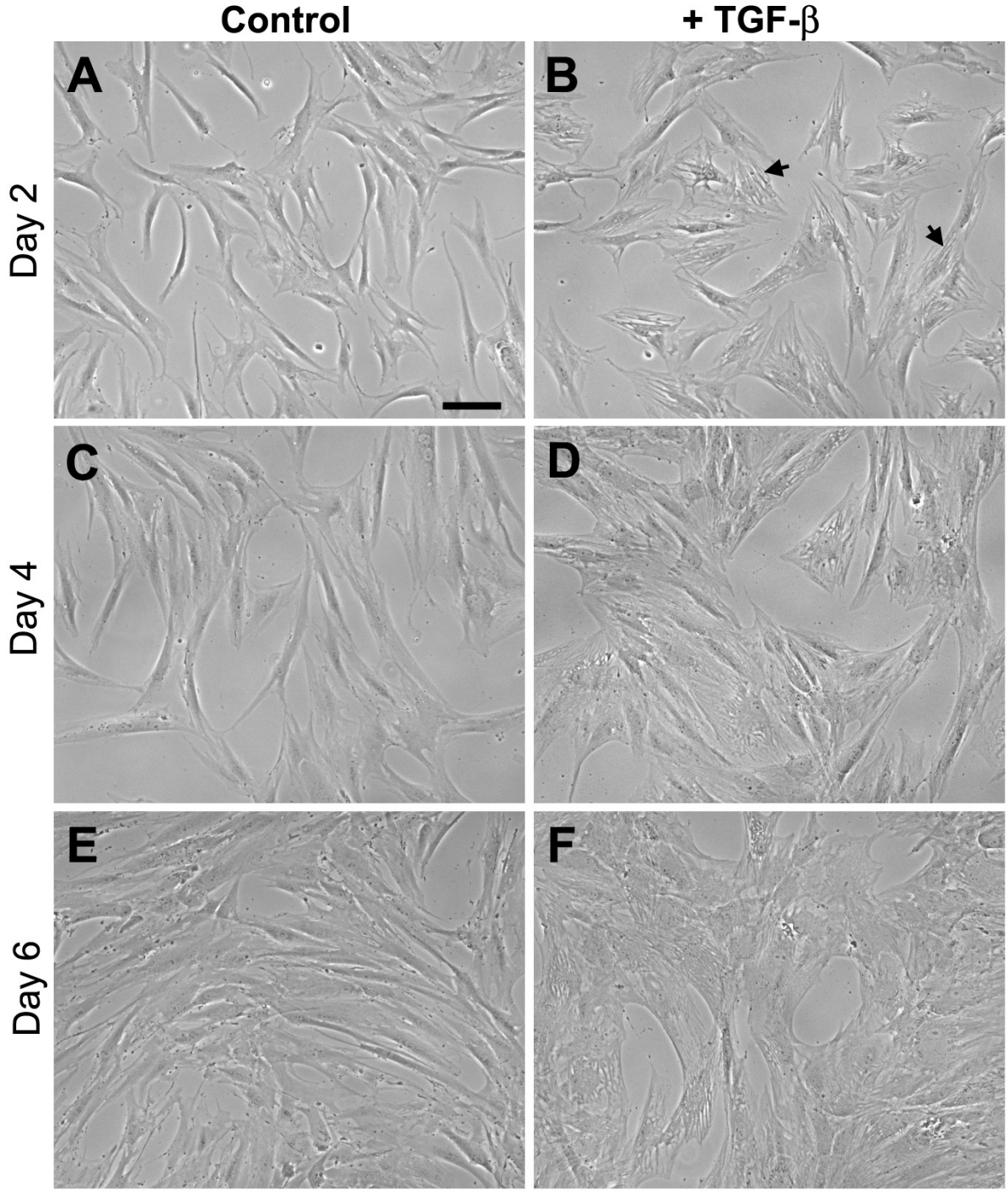

Figure 2

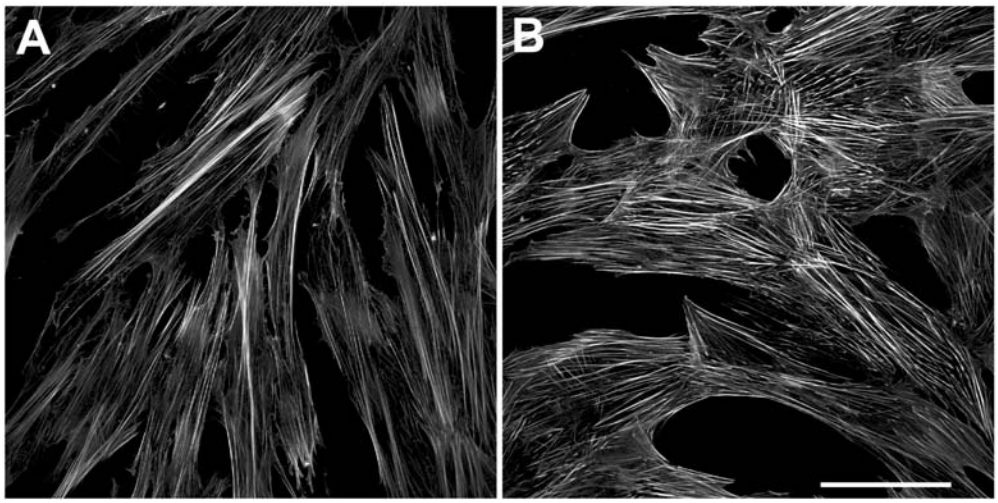
A
B

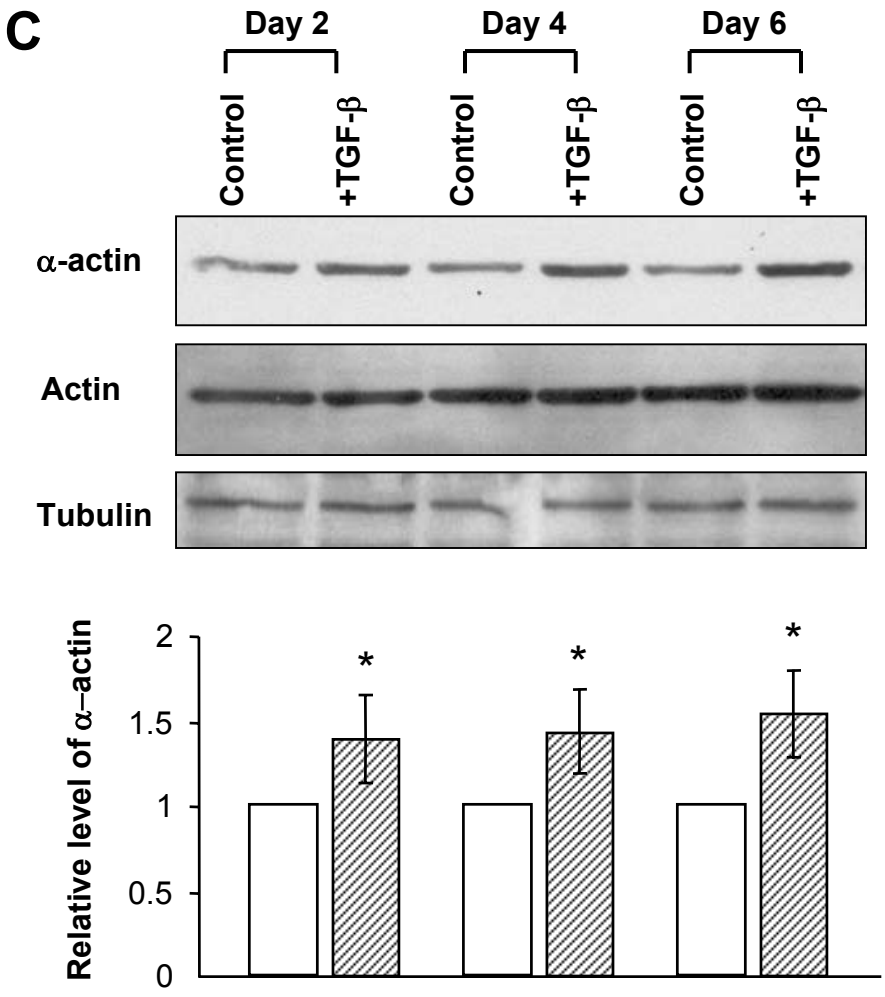
C
Day 2
Day 4
Day 6
Control
+TGF-β
Control
+TGF-β
Control
+TGF-β
α-actin
Actin
Tubulin
Relative level of α–actin
2
1.5
1
0.5
0
*
*
*

Figure 3

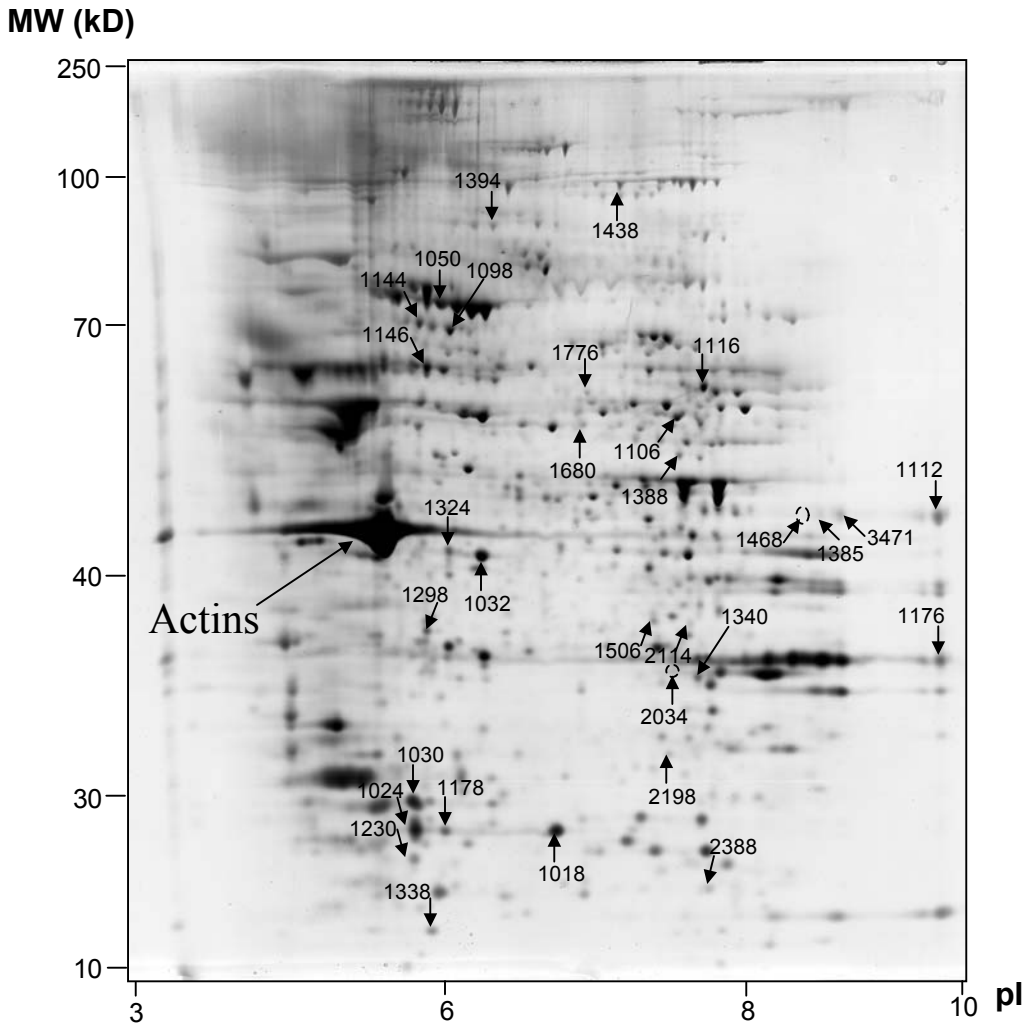
MW (kD)
250
100
70
40
30
10
3
6
8
10
pI
1394
1438
1050
1098
1144
1146
1776
1116
1106
1680
1388
1112
1324
1468
3471
1385
Actins
1298
1032
1340
1176
1506
2114
2034
1030
1024
1178
2198
1230
2388
1018
1338

Figure 4

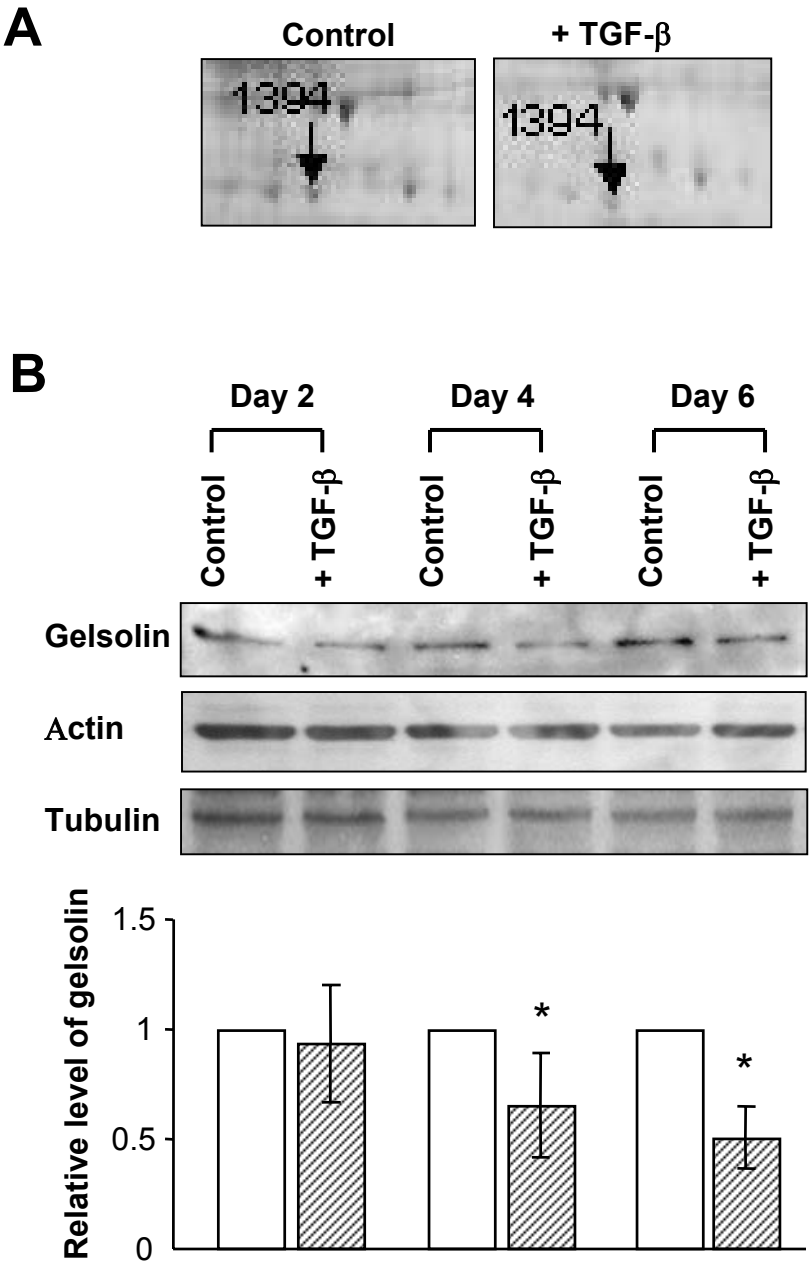
A
Control
+ TGF-β
1394
1394
B
Day 2
Day 4
Day 6
Control
+ TGF-β
Control
+ TGF-β
Control
+ TGF-β
Gelsolin
Actin
Tubulin
Relative level of gelsolin
1.5
1
0.5
0
*
*

Figure 5

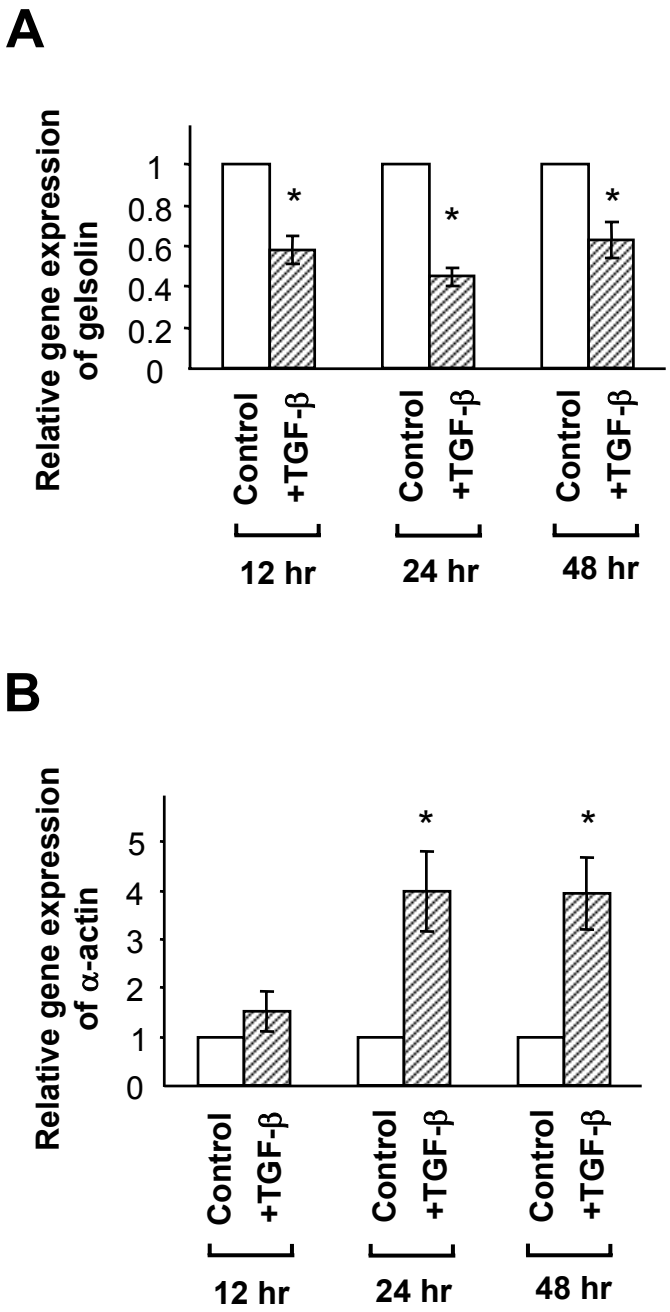
A
Relative gene expression of gelsolin
1
0.8
0.6
0.4
0.2
0
*
*
*
Control
+TGF-β
Control
+TGF-β
Control
+TGF-β
12 hr
24 hr
48 hr
B
Relative gene expression of α-actin
5
4
3
2
1
0
*
*
Control
+TGF-β
Control
+TGF-β
Control
+TGF-β
12 hr
24 hr
48 hr

Figure 6

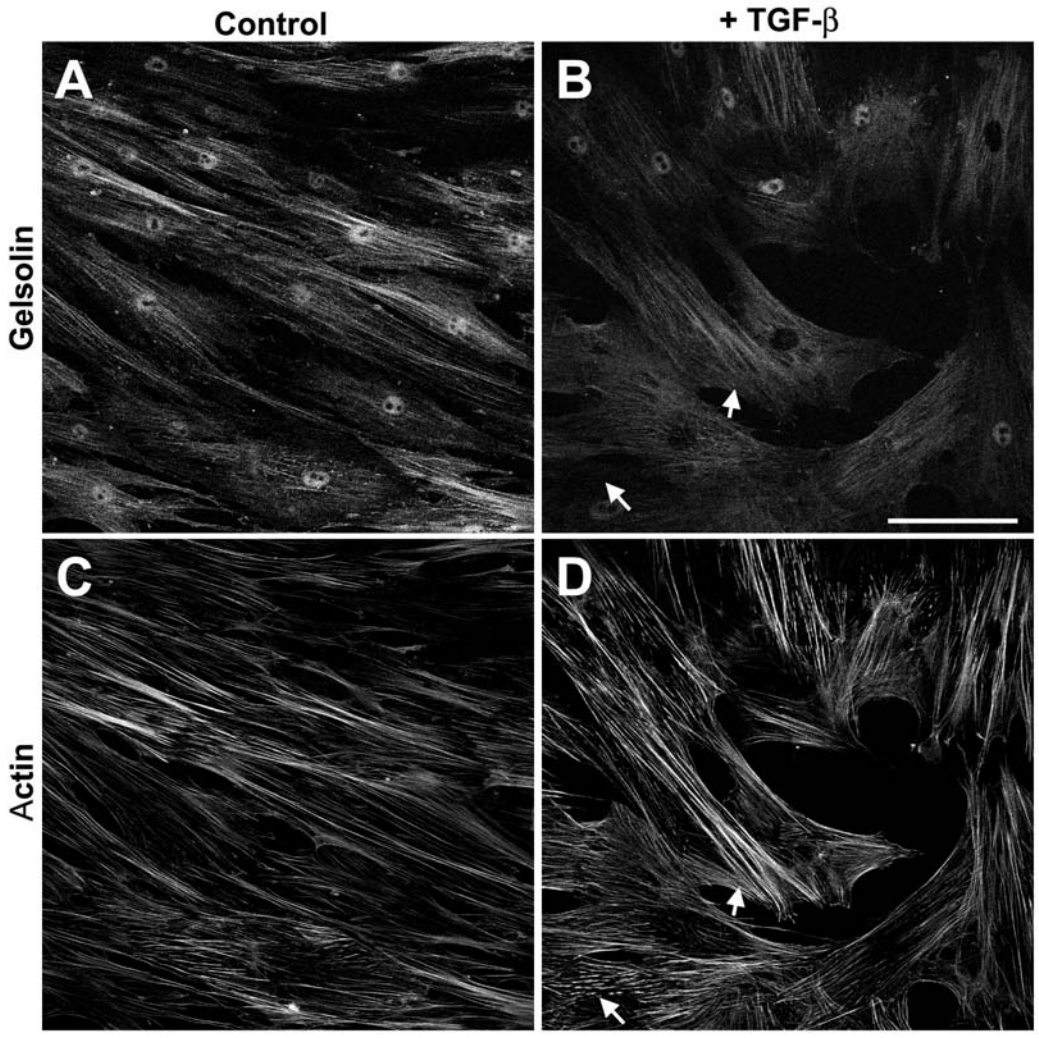

Figure 7

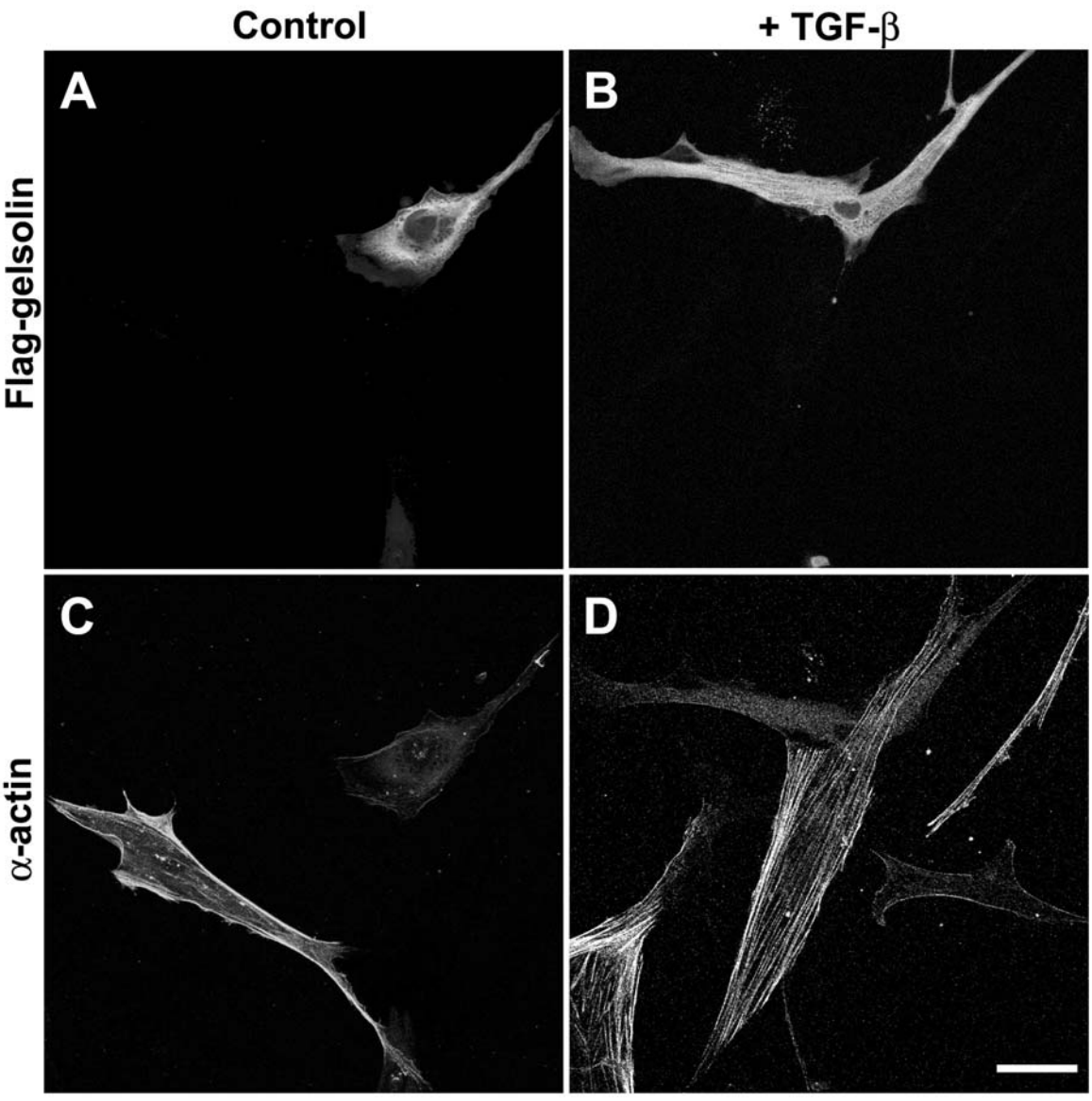

Figure 8

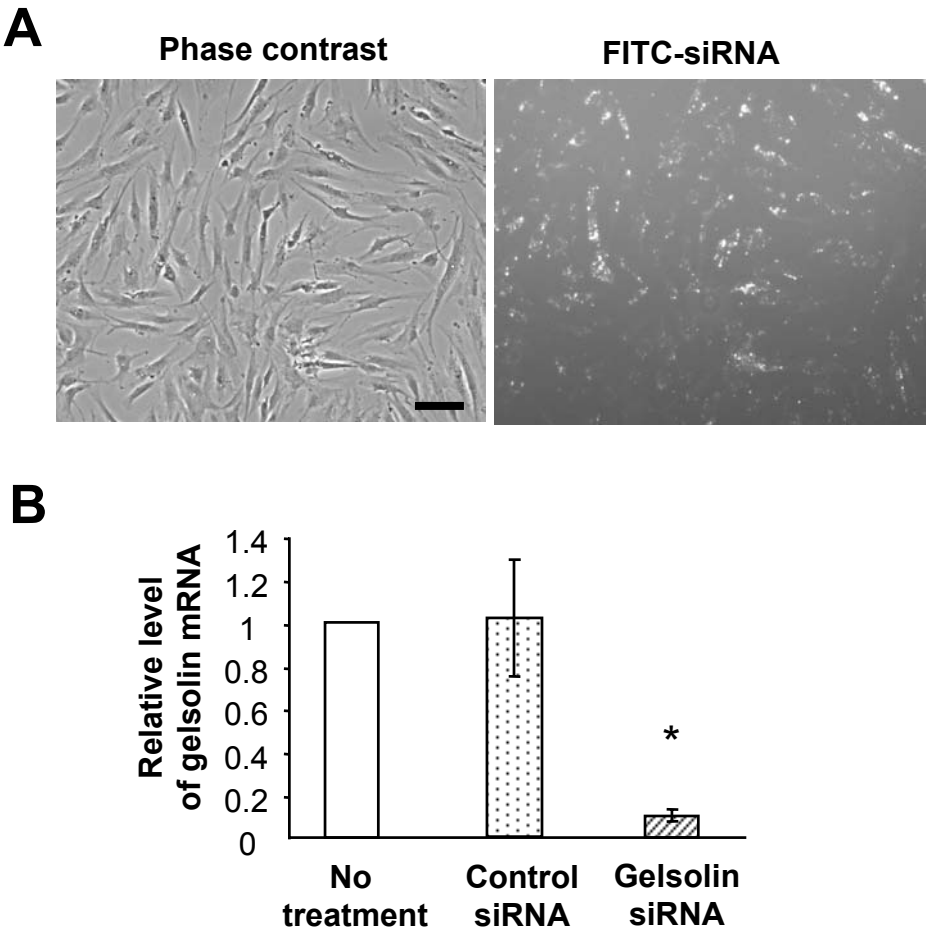
A
Phase contrast
FITC-siRNA
B
Relative level of gelsolin mRNA
1.4
1.2
1
0.8
0.6
0.4
0.2
0
*
No treatment
Control siRNA
Gelsolin siRNA
C
Day 2
Day 4
Day 6
Gelsolin
α-actin
No treatment
Control siRNA
Gelsolin siRNA
No treatment
Control siRNA
Gelsolin siRNA
No treatment
Control siRNA
Gelsolin siRNA

Figure 9

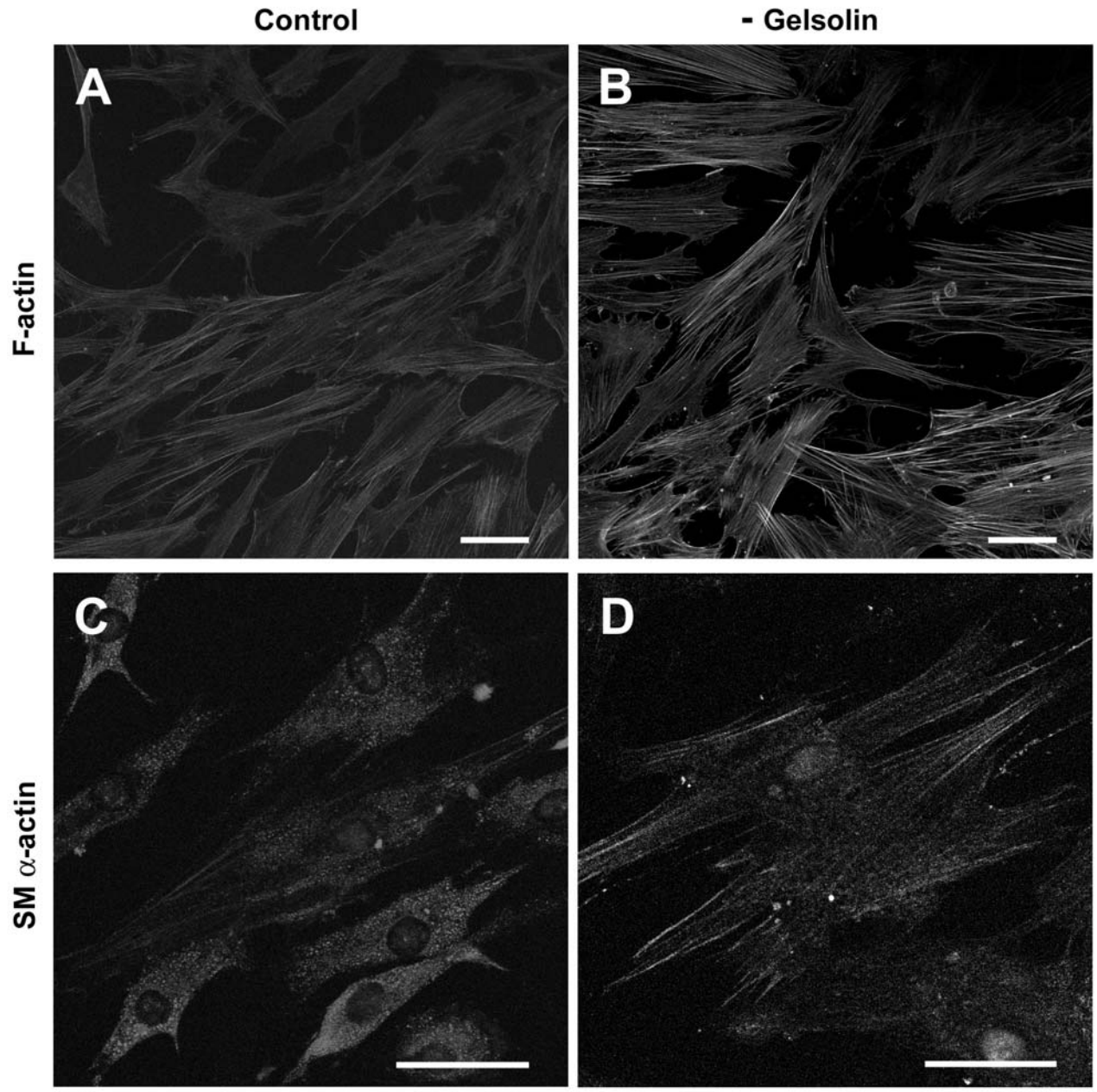

Figure 10